Nanostructures

DOI: 10.1002/anie.201101632

Generation of Hot Spots with Silver Nanocubes for Single-Molecule Detection by Surface-Enhanced Raman Scattering**

*Matthew Rycenga, Xiaohu Xia, Christine H. Moran, Fei Zhou, Dong Qin, Zhi-Yuan Li, and Younan Xia**

Surface-enhanced Raman scattering (SERS) is a near-field phenomenon that relies on the intensified electric fields (E-fields) on a metal nanostructure when its localized surface plasmon resonance (LSPR) is excited by light.[1,2] Although it has been demonstrated that the hot spots between two or multiple Ag nanoparticles can amplify Raman signals by as much as 10^{10} times for single-molecule detection,[3] those hot spots are typically difficult to fabricate and/or troubled by irreproducible performance. Herein we report a novel approach to the fabrication of hot spots with strong and reproducible SERS enhancement factors that simply involves deposition of individual Ag nanocubes on a Ag or Au substrate.[4–8] Our experimental and simulation results indicate that hot spots are created at the Ag nanocube corner sites that are in proximity with the metal substrate, where the E-fields can be enhanced to such a scale that they are capable of detecting SERS from a single molecule. Our approach, while mechanistically similar to the formation of a hot spot in the gap region between two Ag nanoparticles,[9,10] depends only on the deposition of Ag nanocubes on a metal surface. This approach requires minimum fabrication efforts and offers great simplicity for the formation of fully accessible and robust hot spots, thus providing an effective SERS platform for single-molecule detection.

The enhancement factor (EF) of a SERS substrate can be increased by many orders of magnitude because of the formation of hot spots, which are extremely small regions with drastically intensified E-fields.[1] In recent years, the phenomenon of hot spots has been a subject of theoretical studies,[3,10] which have not only confirmed the experimental evidence for the existence of hot spots, but also revealed their subtle dependence on a number of parameters. However, experimental studies and systematic engineering of hot spots have been met with limited success.[11–13] Over the past decade, two strategies have emerged which can generate hot spots at the tip of a sharp feature on a nanoparticle by taking advantage of the lightening rod effect[14] or in the gap region between two closely spaced nanoparticles because of the coupling of plasmon modes.[15] In both cases, the hot spots were formed at known sites and had SERS EFs up to 10^8 for the sharp features on a nanoparticle and 10^{10} for the gap region between two Ag nanoparticles.[16] Larger aggregates of Ag nanoparticles also demonstrated hot spots with enhancement factors (on the order of 10^{14}) sufficiently high to enable single-molecule detection.[3,17] However, formation of such hot spots reproducibly and in large quantities still suffer from the complexity of a salt-induced aggregation or self-assembly process, as well as the difficulty in bringing two nanoparticles together to form a gap with a well-defined distance of only a few nanometers. For these reasons, the aggregation of two or more metal nanoparticles is expected to continue to be unsuccessful as a simple, reproducible, and robust strategy for generating SERS hot spots.

Herein, we report a novel approach for the generation of hot spots with sufficiently strong SERS enhancements for single-molecule detection by simply depositing Ag nanocubes on the surface of an Au or Ag substrate. Specifically, when a Ag nanocube is placed on an Au or Ag substrate, hot spots will be created at the corner sites of the nanocube that are in proximal contact with the metal substrate. While this approach is mechanistically similar to the formation of a hot spot between two closely spaced Ag (or Au) nanoparticles, it only relies on the proximal contact between a nanocube and a metal substrate, which automatically forms during the cast deposition of nanocubes onto a substrate. In addition to simplicity and reproducibility, this new approach offers a great potential to produce SERS substrates with robust, fully accessible hot spots for ultrasensitive detection.

We first validated the formation of hot spots by measuring the SERS EFs of individual Ag nanocubes deposited on different types of substrates. In a typical experiment, we functionalized the surface of Ag nanocubes with 1,4-benzenedithiol (1,4-BDT), deposited them on a substrate, and then recorded the SERS spectra from single particles at 514 nm excitation. After the SERS measurements, we used SEM to obtain information about the size, shape, and orientation of each particle in a process known as SERS-SEM correlation.[18] Figure 1a shows typical SERS spectra taken from Ag nanocubes that were supported on a thermally evaporated thin

[*] M. Rycenga,[+] X. Xia,[+] C. H. Moran, Prof. Y. Xia
Department of Biomedical Engineering, Washington University
St. Louis, MO 63130 (USA)
E-mail: xia@biomed.wustl.edu
F. Zhou, Prof. Z.-Y. Li
Institute of Physics, Chinese Academy of Sciences
Beijing 100080 (P. R. China)
Prof. D. Qin
Department of Energy, Environmental and Chemical Engineering
Washington University, St. Louis, MO 63130 (USA)
[+] These authors contributed equally to this work.

[**] This work was supported in part by a research grant from the NSF (DMR-0804088) and a 2006 Director's Pioneer Award from the NIH (DP1 OD000798). Part of the research was performed at the Nano Research Facility, a member of the National Nanotechnology Infrastructure Network (NNIN), which is supported by the NSF under ECS-0335765.

Supporting information for this article is available on the WWW under http://dx.doi.org/10.1002/anie.201101632.

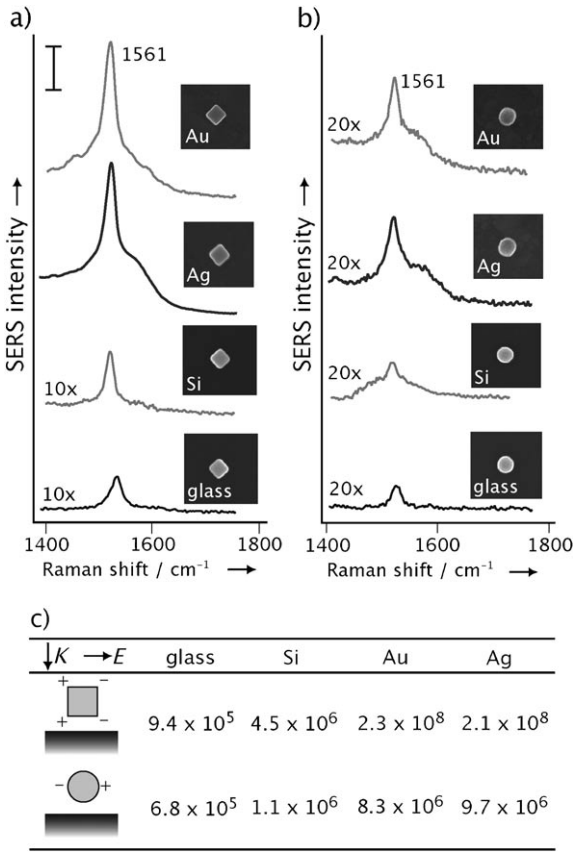

Figure 1. The SERS spectra of 1,4-BDT from: a) nanocubes (106 ± 5) nm in edge length and b) nanospheres (97 ± 7) nm in diameter, on an Au film, Ag film, Si wafer, and glass cover slip, respectively. The insets show their corresponding SEM images. The scale bar for the SERS spectra is 10 adu $mW^{-1} s^{-1}$. c) The EFs for single Ag nanocubes and nanospheres, respectively, supported on different substrates. Each value reported in this table represents an average of the data from 40 particles. The cartoon shows propagation and polarization directions of the laser used in this study and simplified distribution of dipolar charges on each type of particle.

film of gold (Au), a thermally evaporated thin film of silver (Ag), a polished silicon wafer (Si), and a glass cover slip (glass), respectively. The evaporated films were roughly 100 nm thick, with a root-mean-square surface roughness of approximately 5 nm. Since the SERS signals from a Ag nanocube had a strong dependence on its orientation relative to laser polarization,[19] all the spectra reported herein were recorded with its side diagonal or [110] axis aligned parallel to the laser polarization. We recorded the strongest SERS peaks when the Ag nanocubes were supported on a metal substrate and the weakest for those on a glass cover slip. It is worth pointing out that the SERS spectra showed very little variation between different Ag nanocubes supported on the same type of substrate (Figure S1 in the Supporting Information), thus indicating high reproducibility of this new system. For comparison, we also conducted similar SERS measurements with Ag nanospheres whose diameter was approximately the same as the edge length of the nanocubes (Figure 1b). The SERS EFs measured for both Ag nanocubes and nanospheres on different substrates are summarized in Figure 1c. For nanocubes, the EF increased from 9.4×10^5 to 2.3×10^8, that is, by a factor of approximately 250, when the substrate was merely switched from glass to Au or Ag. Note that the EF value reported here corresponds to all the probe molecules on the entire surface of an Ag nanocube. The molecules at the hot spots are supposed to experience EFs that are orders of magnitude higher. The extraordinarily strong enhancement suggests the formation of hot spots when a Ag nanocube was brought into proximal contact with a metal surface. In contrast, the EF was only increased by a factor of 120 for the Ag nanospheres as the substrate was changed from glass to Au or Ag. This observation suggests that the formation of hot spots between a Ag nanoparticle and its supporting substrate is very sensitive to both the shape of the particle and the electrical property of the substrate. In other words, hot spots are only generated when a Ag nanoparticle with sharp corners is brought into contact with a metal surface.

The hot spots are likely formed at the corner sites of a Ag nanocube in proximity with the metal surface rather than those corners away from the substrate. We validated this hypothesis by plasma etching.[20] As shown in Figure 2a, plasma etching should remove all the SERS molecules from the entire surface of an Ag nanocube except the interface region between the nanocube and substrate. We can elucidate the positions of the hot spots by simply comparing the SERS spectra taken from the same Ag nanocube before and after plasma etching. If the hot spots are located at the nanocube–substrate interface, plasma etching should only cause a minor reduction of the SERS intensities, as the number of molecules at the hot spots is not expected to change considerably.[21] On the contrary, if hot spots are not formed, or the hot spots are located at sites away from the nanocube–substrate interface, plasma etching is expected to remove a majority of the molecules and thus attenuate the SERS intensities. As shown in Figure 2b–d, plasma etching attenuated the SERS peak of 4-methylbenzene thiol (4-MBT) at 1592 cm^{-1} by 96%, 76%, and 43%, respectively, when the Ag nanocubes were supported on glass, Si, and Au substrates. In this experiment, we used Au microplates (Figure S2) as the metal substrates because they were more robust under plasma etching than the evaporated films. The data in Figure 2b indicates that the molecules at the nanocube–glass interface did not contribute significantly to the SERS signals, thus implying the absence of hot spots in this system. For nanocubes on Si, approximately 24% of the SERS signals remained after plasma etching (Figure 2c). This data also indicates the absence of intense hot spots capable of single-molecule SERS in this system because the reduction in SERS intensity was more or less proportional to the reduction in number of molecules on the surface. For the Au substrate, however, approximately 57% of the SERS intensity remained after plasma etching (Figure 2d). In this case, approximately 80% of the 4-MBT molecules should have been removed during plasma etching. As a result, the remaining strong SERS peaks provide a clear evidence to support our claim that a relatively small number of molecules on the nanocube were positioned in the hot spots at the nanocube–substrate interface. This data, along with the large SERS EFs derived for Ag nanocubes on Au or Ag

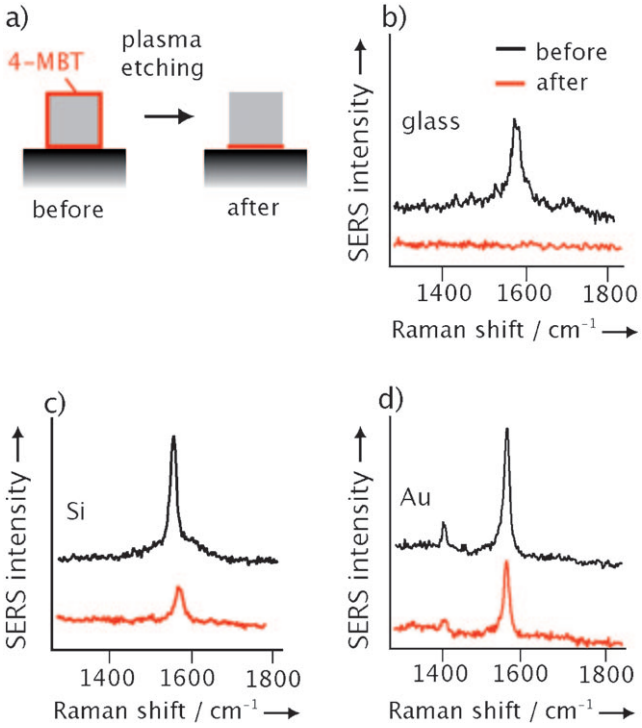

Figure 2. a) Selective removal of 4-MBT molecules (red) from the surface of a Ag nanocube supported on a substrate. Plasma etching with O_2 can remove the exposed molecules on the particle's surface, leaving behind molecules at the nanocube–substrate interface. SERS spectra taken from Ag nanocubes functionalized with 4-MBT (with a peak at 1592 cm^{-1}) and then deposited on b) glass, c) Si, and d) on Au microplate substrates. The SERS spectra were recorded from the same nanocube before and after plasma etching.

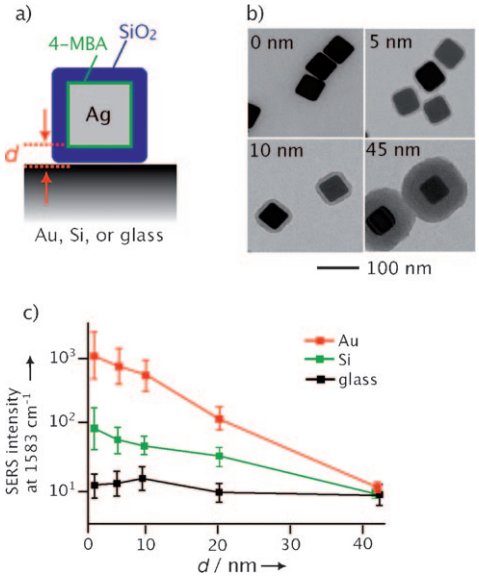

Figure 3. a) Schematic showing how the gap distance (d) between a Ag nanocube and its underlying substrate is controlled by the thickness of the SiO_2 shell (blue). The nanocube was functionalized with SERS-active 4-MBA (green) prior to coating with SiO_2. b) TEM images of Ag nanocubes coated with SiO_2 shells of 0, 5, 10, and 45 nm, respectively, in thickness. c) Plots of SERS peak intensity as a function of thickness for the SiO_2 shell. The peak intensities at 1583 cm^{-1} were recorded for the 4-MBA molecules on single nanocubes supported on Au film, Si wafer, and glass substrates, respectively.

substrates (Figure 1), clearly demonstrates the formation of hot spots at the nanocube–metal interface with exceptionally strong enhancements.

We also examined how the hot spots between a Ag nanocube and its supporting substrate change as the gap distance between them is varied. As shown in Figure 3a, we can easily tune the gap distance (d) between a Ag nanocube and its supporting substrate by coating the nanocube with a dielectric shell of SiO_2. In this case, the surfaces of Ag nanocubes were derivatized with 4-mercaptobenzoic acid (4-MBA, the SERS probe) and then coated with SiO_2 shells of different thicknesses. The plot in Figure 3c shows that, for both the Au and Si substrate, the intensity of the SERS peak of 4-MBA at 1583 cm^{-1} was reduced as the value of d was increased from 0 to 45 nm, while there were very little changes in SERS intensity for the samples supported on glass. In comparison to the EF values in Figure 1c, the system with the largest EF was most sensitive to the value of d. For both dielectric and metal substrates, the interaction of the plasmon modes of the nanoparticle with the substrate will attenuate as the gap distance between the nanoparticle and the substrate increases.[22,23] This data suggests that the near-fields of the Ag nanocube were affected by its supporting substrate, thus resulting in an additional SERS enhancement and formation of hot spots.

To gain a better understanding of the hot spots formed between a Ag nanocube and its supporting substrate, we used the discrete dipole approximation (DDA) method to calculate the distributions of E-field enhancement (Figure 4a). We performed simulations for both nanocubes and nanospheres supported on Au and Si substrates, respectively, as well as suspended in air. The distributions of E-field enhancement (Figure 4) are consistent with the trends of SERS EFs experimentally obtained for the nanoparticles supported on different types of substrates (Figure 1c). The largest E-field enhancement occurs for the nanocube on Au and is highly localized at the corner sites (Figure 4c). For a nanosphere, although its E-fields are enhanced on Au compared with Si and air, hot spots are not formed. The experimental and DDA simulations clearly show that the substrate can influence the E-fields of metal nanoparticles and cause further increase to their SERS EFs. However, there has been little investigation into how the substrate affects the SERS of a supported particle, and the exact mechanism behind particle–substrate interactions remains unknown. For nonmetal substrates, a nanoparticle can induce image charges in the substrate, which then interact with the nanoparticle's plasmon modes.[24–26] In contrast, a metal substrate can support propagating surface plasmon (PSP) modes, which can hybridize with the nanoparticle's LSPR, thus resulting in plasmon gap modes[27,28] and generation of huge local E-field enhancements.[7,29–31] Theoretical calculations suggest that, like a dimer of metal nanoparticles, the dielectric gap between the metal nanoparticle and the metal substrate may be critical to the formation of enhanced local E-fields.[25,31] The large increase

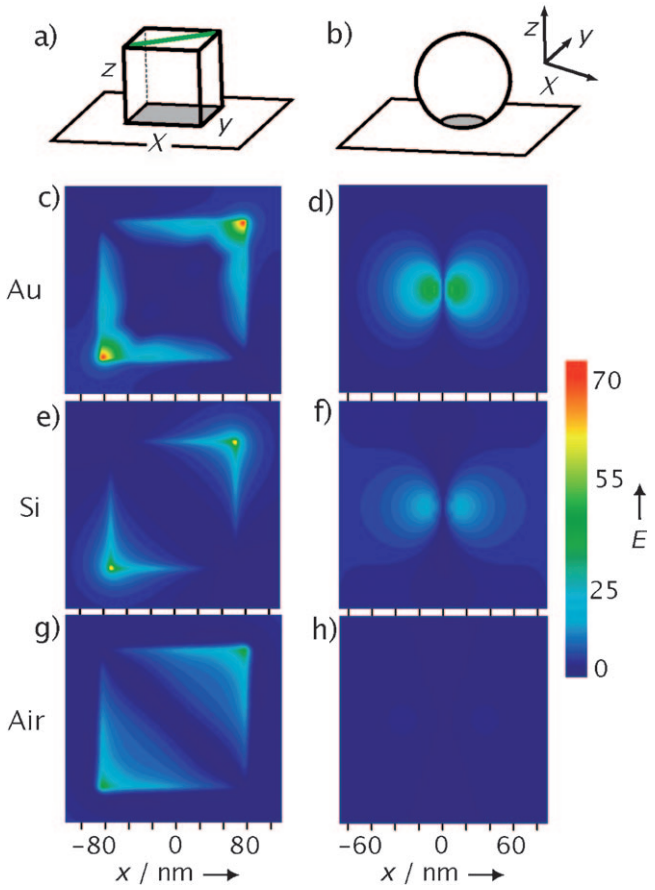

Figure 4. Simulated E-field enhancements for a Ag nanocube or nanosphere. a, b) Coordination systems for calculating the E-field enhancement distribution of a nanocube and nanosphere, respectively, positioned 2 nm above a substrate. The gray region represents the plane plotted in the simulations and is 1 nm above the underlying substrate. For nanocubes, the polarization was along the green line. The E-field enhancement distributions calculated using the DDA method for: nanocubes c) on Au, e) on Si, and g) in air; as well as for nanospheres d) on Au, f) on Si, and h) in air.

in SERS EF for a nanocube on a metal substrate is evidence for this strong interaction. Unlike glass or Si, the metal substrate can couple with the LSPR of the nanocube and significantly enhance its E-fields.

Since the SERS EFs measured for single nanocubes on a metal substrate were in the order of 10^8 at 514 nm excitation, their hot spots should allow for the detection of single molecules under resonant conditions.[32] The use of a single nanoparticle for single-molecule detection has not received much attention, and when it has, often through simulations, a contacting substrate was never taken into consideration.[16] Single-molecule detection with SERS has benefited greatly from the demonstration of a bianalyte technique that uses two different molecules in equal concentrations as the SERS probes.[3,12] This technique avoids the use of methods of simply diluting the probe molecules to ultralow concentrations in order to demonstrate single-molecule sensitivity. In this new technique, the majority of the SERS spectra should contain both types of molecules unless a hot spot is involved, then the spectrum will be dominated by only one type of molecules at the hot spot. In a typical experiment, both rhodamine 6G (R6G) and crystal violet (CV) dyes (100 nM) were incubated with the Ag nanocubes (at a ratio of approximately 500 molecules per nanocube) that were subsequently deposited onto a thermally evaporated film of Ag for SERS measurements. Figure 5a shows a dark-field optical

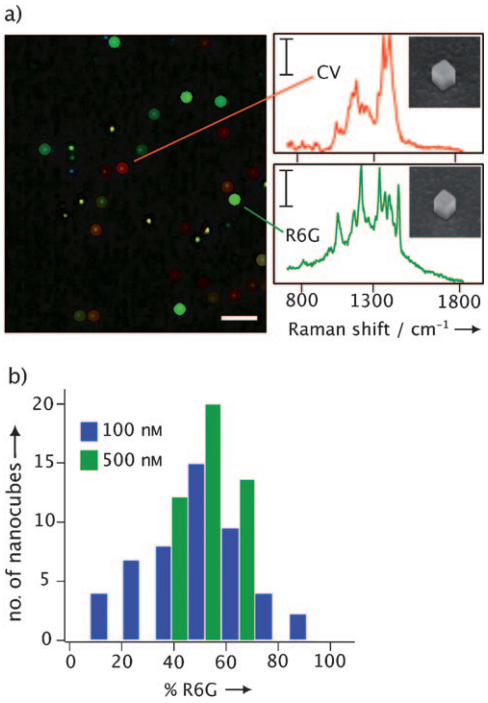

Figure 5. a) Dark-field optical micrograph of Ag nanocubes on a Ag film, with a SERS color map overlay to mark the SERS spectra uniquely from CV (red) or R6G (green). The other colors indicate that the spectra were a combination of both dyes. The scale bars for the dark-field image and SERS spectra are 10 μm and 8 adu mW^{-1} s^{-1}, respectively. The inset shows SEM images (at a tilt angle of 45°) of the nanocubes from which the two spectra were recorded. b) Histogram of the percentage the SERS spectrum from a nanocube was characterized as R6G (P_{R6G}) at concentrations of 100 nM and 500 nM. The SERS spectra were acquired with 514 nm excitation, 1 s acquisition, and 0.5 mW laser power.

micrograph with a color-map overlay indicating spectra unique to R6G (red) and CV (green), recorded with 514 nm excitation and an acquisition time of 1 s. The two spectra unique to R6G and CV are also shown, together with SEM images of the two corresponding Ag nanocubes. The histogram in Figure 5b shows a distribution of the spectra recorded from single nanocubes and the percentage the spectrum was characterized as R6G (P_{R6G}).[12] At $P_{R6G} = 100\,\%$, the spectrum would be representative of only R6G, and at $P_{R6G} = 0\,\%$ the spectrum would be only CV. Because each nanocube had approximately 500 molecules of both dyes on it, the spectrum recorded from a nanocube should be a combination of both molecules and the data should be concentrated at $P_{R6G} \approx 50\,\%$ (Figure 5b). This was not the case, however, and some nanocubes showed spectra that were dominated by R6G or CV, thus indicating that these spectra originated from only a few molecules positioned in the areas of the highest enhance-

ments or the hot spots. With a higher concentration of R6G and CV, the single molecule spectra should become less evident, as more molecules would decrease the probability of positioning only a few molecules at the hot spots. This effect is exactly what we observed when the concentration was increased to 500 nM and the spectra from individual nanocubes were representative of both types of molecules. The existence of two hot spots between the nanocube and its supporting substrate, and our limited data set (50 nanocubes were probed), make it difficult to conclude that the spectrum originated from one molecule only (two molecules might have contributed to the signal, for example). However, to the best of our knowledge, this is the first demonstration of SERS detection on the single-molecule level with a single Ag nanoparticle, and many parameters stand to be optimized including the excitation wavelength, as well as the thickness and roughness of the metal substrate.

In conclusion, by varying the shape of an Ag nanoparticle, the electrical property of a substrate, the spatial location of probe molecules on the nanoparticle, and the gap distance between the nanoparticle and its supporting substrate, we have collected experimental evidence to support the formation of hot spots between an Ag nanocube and an Au or Ag surface. This new type of hot spot offers a number of advantages over the conventional hot spots between two closely spaced nanoparticles: 1) the Ag nanocubes can be routinely synthesized with good uniformity in terms of shape and size distributions,[33] and they can be prepared with sharp corners and relatively large dimensions to ensure much stronger SERS enhancements relative to their smaller or rounded counterparts; 2) the proximal contact between an Ag nanocube and a metal substrate is almost guaranteed to form during the cast deposition process; and 3) the hot spots are created at the corner sites around an Ag nanocube rather than between the side face of a nanocube and its supporting substrate, thus making the hot spots fully accessible by a potential analyte of any size. We believe this strategy is highly adaptable to different types of nanoparticles and substrates, and represents a new, general direction in the design of SERS hot spots in contrast to the formation of nanoparticle dimers or other complex structures.

Received: March 5, 2011
Published online: May 3, 2011

Keywords: nanostructures · silver · single-molecule detection · surface-enhanced Raman scattering · surface plasmon resonance

[1] C. L. Haynes, A. D. McFarland, R. P. Van Duyne, *Anal. Chem.* **2005**, *77*, 338A.
[2] E. L. Ru, P. Etchegoin, *Principles of Surface Enhanced Raman Spectroscopy*, Elsevier, **2009**.
[3] J. A. Dieringer, R. B. Lettan, K. A. Scheidt, R. P. Van Duyne, *J. Am. Chem. Soc.* **2007**, *129*, 16249.
[4] M. K. Kinnan, G. Chumanov, *J. Phys. Chem. C* **2007**, *111*, 18010.
[5] K. Kim, J. K. Yoon, *J. Phys. Chem. B* **2005**, *109*, 20731.
[6] J. D. Driskell, R. J. Lipert, M. D. Porter, *J. Phys. Chem. B* **2006**, *110*, 17444.
[7] I. Yoon, T. Kang, W. Choi, J. Kim, Y. Yoo, S.-W. Joo, Q.-H. Park, H. Ihee, B. Kim, *J. Am. Chem. Soc.* **2009**, *131*, 758.
[8] G. Braun, S. J. Lee, M. Dante, T.-Q. Nguyen, M. Moskovits, N. Reich, *J. Am. Chem. Soc.* **2007**, *129*, 6378.
[9] W. Li, P. H. C. Camargo, L. Au, Q. Zhang, M. Rycenga, Y. Xia, *Angew. Chem.* **2010**, *122*, 168; *Angew. Chem. Int. Ed.* **2010**, *49*, 164.
[10] L. Qin, S. Zou, C. Xue, A. Atkinson, G. C. Schatz, C. A. Mirkin, *Proc. Natl. Acad. Sci. USA* **2006**, *103*, 13300.
[11] E. LeRu, E. Blackie, M. Meyer, P. G. Etchegoin, *J. Phys. Chem. C* **2007**, *111*, 13794.
[12] E. LeRu, M. Meyer, P. G. Etchegoin, *J. Phys. Chem. B* **2006**, *110*, 1944.
[13] E. LeRu, P. G. Etchegoin, *Chem. Phys. Lett.* **2006**, *423*, 63.
[14] P. Senthil Kumar, I. Pastoriza-Santos, B. Rodriguez-Gonzalez, F. J. G. de Abajo, L. M. Liz-Marzan, *Nanotechnology* **2008**, *19*, 015606.
[15] X. Zhang, N. C. Shah, R. P. Van Duyne, *Vib. Spectrosc.* **2006**, *42*, 2.
[16] E. Hao, G. C. Schatz, *J. Chem. Phys.* **2004**, *120*, 357.
[17] M. J. Banholzer, J. E. Millstone, L. Qin, C. A. Mirkin, *Chem. Soc. Rev.* **2008**, *37*, 885.
[18] M. Rycenga, P. H. C. Camargo, W. Li, C. H. Moran, Y. Xia, *J. Phys. Chem. Lett.* **2010**, *1*, 696.
[19] J. McLellan, Z.-Y. Li, A. Siekkinen, Y. Xia, *Nano Lett.* **2007**, *7*, 1013.
[20] C. Chatgilialoglu, M. D'Angelantonio, M. Guerra, P. Kaloudis, Q. G. Mulazzani, *Angew. Chem.* **2009**, *121*, 2248; *Angew. Chem. Int. Ed.* **2009**, *48*, 2214.
[21] Y. Fang, N.-H. Seong, D. D. Dlott, *Science* **2008**, *321*, 388.
[22] J. J. Mock, R. T. Hill, A. Degiron, S. Zauscher, A. Chilkoti, D. R. Smith, *Nano Lett.* **2008**, *8*, 2245.
[23] W.-H. Park, S.-H. Ahn, Z. H. Kim, *ChemPhysChem* **2008**, *9*, 2491.
[24] J. M. McMahon, Y. Wang, L. J. Sherry, R. P. Van Duyne, L. D. Marks, S. K. Gray, G. C. Schatz, *J. Phys. Chem. C* **2009**, *113*, 2731.
[25] Y. Wu, P. Nordlander, *J. Phys. Chem. C* **2010**, *114*, 7302.
[26] M. W. Knight, Y. Wu, J. B. Lassiter, P. Nordlander, N. J. Halas, *Nano Lett.* **2009**, *9*, 2188.
[27] J. K. Yoon, K. Kim, K. S. Shin, *J. Phys. Chem. C* **2009**, *113*, 1769.
[28] C. J. Orendorff, A. Gole, T. K. Sau, C. J. Murphy, *Anal. Chem.* **2005**, *77*, 3261.
[29] P. Nordlander, E. Prodan, *Nano Lett.* **2004**, *4*, 2209.
[30] F. Le, N. Z. Lwin, J. M. Steele, M. Kall, N. J. Halas, P. Nordlander, *Nano Lett.* **2005**, *5*, 2009.
[31] G. Lévêque, O. J. F Martin, *Opt. Express* **2006**, *14*, 9971.
[32] J. P. Camden, J. A. Dieringer, Y. Wang, D. J. Masiello, L. D. Marks, G. C. Schatz, R. P. Van Duyne, *J. Am. Chem. Soc.* **2008**, *130*, 12616.
[33] Q. Zhang, W. Li, C. Moran, J. Zeng, J. Chen, L.-P. Wen, Y. Xia, *J. Am. Chem. Soc.* **2010**, *132*, 11372.

